

Variable UV Absorption in the Spectrum of MRC 2251–178¹

Rajib Ganguly, Jane C. Charlton, Michael Eracleous

Department of Astronomy and Astrophysics
 The Pennsylvania State University, University Park, PA 16802
 e-mail: `ganguly, charlton, mce@astro.psu.edu`

ABSTRACT

We present an ultraviolet spectrum of MRC 2251–178 taken with HST/STIS-G230L. The observation is part of a snap shot program of QSOs to systematically search for intrinsic absorption lines through variability. The sample consists of all QSOs observed with HST/FOS which showed associated narrow absorption lines. The FOS spectrum of MRC 2251–178, taken in 1996, showed an associated C IV doublet with an $\lambda 1548$ equivalent width 1.09 ± 0.09 Å (Monier et al. 2001). It is not detected in the STIS spectrum taken four years later, down to a 3σ threshold of 0.19 Å. In addition to its other accolades, these observations make MRC 2251–178 the very first QSO at low redshift in which the associated absorption is shown to be truly intrinsic. We discuss the implications of this and suggest courses for future study.

Subject headings: quasars: absorption lines – quasars: individual (MRC 2251-178)

1. Introduction

The identification of QSO-intrinsic narrow absorption lines² has exploded over the past four years with the advent of high resolution spectroscopy with large ground-based telescopes. With this explosion has come new insights on how to identify these absorbing systems - that is, how to separate them from randomly distributed intervening material. Historically, large ensembles of intrinsic absorbers have been identified using statistical arguments, either demonstrating an excess of absorbers in some redshift path (Foltz et al. 1986; Anderson et al. 1987) or by correlating the velocity distribution (with respect to the QSO emission redshift) of absorbers with QSO properties

¹Based on observations with the NASA/ESA *Hubble Space Telescope*, obtained at the Space Telescope Science Institute, which is operated by AURA, Inc., under NASA contract NAS 5-26555.

²Hereafter, we abbreviate narrow absorption line with the acronym NAL and refer to a QSO that hosts a truly *intrinsic* NAL as a NALQSO.

(Richards et al. 1999). Such surveys have demonstrated that, in high redshift QSOs, there *is* an excess of absorbers that lie within 5000 km s^{-1} of the QSO emission redshift (termed “associated” absorbers). It is now generally accepted that a large fraction of associated absorbers are indeed intrinsic. However, it is not truly known how large this fraction is. Moreover, Richards et al. (1999) demonstrated that a significant fraction of non-associated (that is, high ejection velocity) absorbers may also be intrinsic.

The two smoking guns, according to Barlow & Sargent (1997), that identify an intrinsic system are: (1) variability of the spectral profiles and/or equivalent widths over time [e.g., Hamann et al. (1995); Barlow et al. (1997); Hamann et al. (1997b,c); Aldcroft et al. (1997)]; and (2) the signature of partial coverage [e.g., Barlow & Sargent (1997); Barlow et al. (1997); Hamann et al. (1997a); Ganguly et al. (1999)]. Thusfar, all cases of confirmed QSO-intrinsic NALs are at high redshift, where the resonant UV doublets of metals are shifted into the optical. At low redshift, Ganguly et al. (2001) estimate from statistical excesses that $\sim 25\%$ of QSOs have intrinsic NALs. As a first step in determining that true fraction of intrinsic NALs, and deciphering the dominant cause of variability (if one exists) we have undertaken an HST/STIS snap shot program to identify intrinsic NALs in a sample of QSOs where associated NALs have been detected in archived HST/FOS spectra. In this effort, we also hope to look for high ejection velocity absorbers at low redshift and decipher the nature of the variability. We note that, up until now, only six QSOs have been shown to host intrinsic absorption through time variability - all at $z_{\text{em}} > 1.5$. Furthermore all cases of associated, time variable absorption have been low luminosity AGN (Walter et al. 1990; Shull & Sachs 1993; Maran et al. 1996; Weymann et al. 1997; Crenshaw et al. 2000).

In this letter, we report the first confirmation at low redshift of an associated NAL that is truly intrinsic to a QSO, MRC 2251–178 [$z_{\text{em}} = 0.066092$; Bergeron et al. (1983)]. The radio-quiet MRC 2251–178 is well-known for having a highly variable X-ray warm absorber, the first one known (Halpern 1984). Monier et al. (2001) first reported an associated UV absorber and, assuming that the same gas produced the X-ray warm absorption, inferred that the mass loss rate from the disk and the accretion rate were comparable.

In §2, we present our HST/STIS snapshot of MRC 2251–178. In §3, we show that the associated UV absorption has varied over the past four years (thus, verifying its intrinsic nature). In §4, we discuss the implications of variability on analyses of intrinsic absorption lines and make suggestions for future work on MRC 2251–178

2. Data

The sample for our snap shot program is drawn from QSOs in the HST/FOS archive. The sample is restricted to only those QSOs which have been observed with one of the “high” resolution ($\sim 230 \text{ km s}^{-1}$) FOS gratings (G130H, G190H, G270H) and for which there is evidence of associated absorption in the form of a C IV $\lambda\lambda 1548, 1550$, N V $\lambda\lambda 1393, 1403$, O VI $\lambda\lambda 1032, 1038$, or Ly α

feature. The sample, comprised of 37 QSOs, includes 13 NALQSO candidates from Ganguly et al. (2001), which derived from a subsample of the *HST Quasar Absorption Line Key Project QSOs*, as well as 24 QSOs which were not part of the Key Project. The QSOs from the Key Project (Bahcall et al. 1993; Schneider et al. 1993; Bahcall et al. 1996; Jannuzi et al. 1998) were obtained from D. Schneider, B. Jannuzi, and S. Kirhakos. The non-Key Project QSOs were reduced and supplied by S. Kirhakos. All QSOs were obtained fully reduced with effective continuum³ fits according to Schneider et al. (1993).

The primary goal of the snap shot program is to detect variability of associated NALs. To that end, the QSOs are observed using HST/STIS with the G230L grating and the $52 \times 0.2''$ slit. The dispersion of the grating is 1.58 \AA per pixel, with two pixels per resolution element. This corresponds to $300\text{--}600 \text{ km s}^{-1}$ across the spectrum, compared to the roughly constant 230 km s^{-1} resolution of the FOS spectra. In Fig 1, we show the full spectrum of MRC 2251-178 (darker histogram) resulting from a 500 s exposure taken on 5 November 2000. The signal-to-noise per pixel at 2376 \AA (the central wavelength) is ~ 25 . The comparison HST/FOS spectrum, also shown in Fig 1 (lighter histogram), was taken on 2 August 1996 with all three 230 km s^{-1} resolution gratings (Monier et al. 2001). The relevant portion of the spectrum (taken with the G190H grating) has a signal-to-noise similar to the STIS spectrum. The flux calibration from the reduction pipelines for both the STIS-G230L and FOS-G190H spectra are accurate to within 3%. The wavelength calibration for the FOS-G190H spectrum is accurate to 0.11 diodes (0.2 \AA) while that of the STIS-G230L spectrum is accurate to 0.2–0.5 pixels ($0.3\text{--}0.8 \text{ \AA}$). A STIS-G140M spectrum, obtained 3 February 1998 by J. Stocke, spans the wavelength range $1194\text{--}1300 \text{ \AA}$ (in two separate grating tilts). Although this spectrum covers the associated absorption from Ly α and N V transitions, there is, unfortunately, no overlap with our STIS-G230L. As a result, no direct comparison can be made to the STIS-G140M spectrum.

3. Analysis & Results

It is apparent by visual inspection of the STIS (Fig. 1) and FOS (Monier et al. 2001: Fig. 1) spectra that there has been a change in the state of both the emission and associated absorption lines of MRC 2251-178. The STIS spectrum has a generally higher flux and the associated C IV absorption has apparently disappeared. To examine the magnitude of the variability, we convolved the FOS spectrum with a Gaussian (575 km s^{-1} FWHM) and resampled the result with a $1.58 \text{ \AA}/\text{pixel}$ dispersion to mimic the expected STIS-G230L spectrum around the C IV emission line.

In Fig. 2, we show the C IV emission and associated absorption lines from the observed FOS

³The effective continuum is the sum of the continuum and broad emission lines from the QSO. It is the spectrum that is presumably incident on the absorbing gas.

spectrum (top panel; solid histogram), and the observed STIS spectrum (bottom panel; solid histogram). Overplotted on each are the effective continuum fits (smooth curve) and the expected STIS spectrum (dotted histograms). In the top panel, the expected STIS spectrum reflects what should have been observed if there were no variability in either the C IV emission or associated absorption lines. In the bottom panel, the expected STIS spectrum shows what should have been observed if there were no change in the properties of the associated absorber (that is, if only the shape of the C IV emission line and the continuum flux changed). With STIS-G230L, the associated C IV absorption is sampled by seven pixels (3.5 resolution elements) and should have been detected in the observed spectrum. (The Galactic Al II line at 1670 Å, which is sampled by less than a pixel in the STIS spectrum, is completely washed out by the instrumental profile, making it indistinguishable from the C IV and He II emission lines.) Furthermore, Monier et al. (2001) measured a C IV λ 1548 equivalent width of 1.09 ± 0.09 Å in the FOS spectrum. Using the unresolved feature detection method from Schneider et al. (1993), the absorber is not formally detected in the STIS spectrum down to a 3σ equivalent width limit of 0.19 Å. This is more than a 10σ change. It is, therefore, clear and robust that there has been variability in the properties of the associated absorber.

4. Discussion

4.1. Variability in the UV spectrum

The change in the state of associated C IV absorption happened sometime in the last four years. Although, we cannot say accurately on what timescale that variability occurred, it is now safe to say that this is the first clear demonstration of truly intrinsic narrow absorption in a low redshift QSO. Variability in absorption lines is generally attributed to one of two scenarios. In the first scenario, bulk motion, the absorption gas has an appreciable motion transverse to the line of sight and the total column density through the gas changes with time. The observational signature is that the equivalent width of all lines due to this gas should change in the same way (that is, all get stronger or all get weaker) with time. In the second scenario, ionization/recombination, the physical state of the absorber changes such that the absorbing gas becomes more or less ionized with time. Observationally, this would mean that the equivalent widths of higher-ionization lines and lower-ionization lines should change in opposite directions. This assumes, however, that the kinematics of the gas does not change so that the column densities of the ions drive the changes in the equivalent widths. Unfortunately, the four year separation of the two UV observations and the lack of coverage of relevant species by the STIS G230L observation (e.g., Ly α , N V $\lambda\lambda$ 1393, 1403, Si IV $\lambda\lambda$ 1394, 1403, Si II λ 1260, C II λ 1335) do not allow one to distinguish between these two causes of the variability in the spectrum of MRC 2251–178.

Nevertheless, since we know that the variability timescale is less than 4 years, we can provide an upper limit on the distance between the absorbing material and the ionizing sources. If we

assume that the cause of variability is recombination of C IV to C III and that the temperature of the absorber is about $T_e = 2 \times 10^5$ K as in UM 675 (Hamann et al. 1995), then the minimum density is $n_e = 1/t_{\text{rec}}\alpha > 3000 \text{ cm}^{-3}$, where the recombination coefficient is $\alpha = 2.8 \times 10^{-12} \text{ cm}^3 \text{ s}^{-1}$ (Arnaud & Rothenglug 1985). This implies a maximum distance of 2.4 kpc, if C IV is the dominant species. This is consistent with the estimate from Monier et al. (2001). While not very restrictive, the distance estimate does rule a number of candidates for the absorbers, including the intergalactic medium of the host cluster and most of the interstellar medium of the host galaxy. The remaining possibilities are the material mixed with broad emission line region (BLR), material outside the BLR, and outflowing/ejected material.

4.2. Suggestions for Future Work

The next step in understanding the intrinsic absorber in MRC 2251–178 is to decipher the cause of variability - bulk motion or ionization/recombination - and then determine if there is a direct physical relationship between the gas and the X-ray warm absorber. In principle, these issues can be tackled, but they require a regimented observing schedule. To efficiently determine both the underlying cause of variability and the geometry of absorbing gas relative to the central engine, periodic observations at medium to high resolution should be obtained of the rest-frame wavelength range 1200–1600 Å (e.g., with the E140M echelle on STIS). This covers transitions of Si II, Ly α , N V, C II, Si IV, and C IV. The frequency of the observations should be less than (or on the order of) once in two months. If the QSO and/or absorber properties vary within the course of observations, this schedule should provide the variability timescale. In addition, at high resolution, photoionization modeling of the individual components should constrain the physical conditions of the gas. Furthermore, measurements of the partial coverage fraction are possible (and necessary) with the resolved components. The combination of the partial coverage fraction, the physical conditions of the gas (e.g. the ionization parameter, density), and the variability timescale can constrain the distance from the central engine, the size, and the transverse velocity of the absorbers.

Once the range of conditions in the UV absorbing gas are known, one can then consider its relationship to the X-ray warm absorber. This, however, is difficult since the X-ray warm absorber is known to vary on short timescales (< 1 year; Halpern 1984). Thus, simultaneous observations of MRC 2251–178 in both the UV and the X-ray are required so that inferred relationships are not affected by the changing conditions. In the X-ray, observations can be carried out with either the Chandra/HETG or XMM-Newton/RGS to cover O VII and O VIII. Ultraviolet observations should be carried out with either HST/STIS-E140M, which covers a range of ionization states, and/or with FUSE, which covers the O VI $\lambda\lambda 1032, 1038$ doublet and the Lyman series.

Support for this work was provided under grants HST-GO-08681.01-A and STSI AR-08763.01-A. We are grateful to Sofia Kirhakos for providing the uniformly and fully reduced FOS archive

with continuum and emission line fits.

REFERENCES

Aldcroft, T., Bechtold, J., & Foltz, C. 1997, in ASP Conference Ser. 128, Mass Ejection from Active Galactic Nuclei, ed. N. Arav, I. Shlosman, & R. Weymann (San Francisco: ASP), 25

Anderson, S. F., Weymann, R. J., Foltz, C. B., & Chaffee, F. H. 1987, AJ, 94, 278

Arnaud, M., & Rothenflug, R. 1985, A&AS, 60, 425

Barlow, T. A., Hamann, F., & Sargent, W. L. W., 1997, in ASP Conference Ser. 128, Mass Ejection from Active Galactic Nuclei, ed. N. Arav, I. Shlosman, & R. Weymann (San Francisco: ASP), 13

Bahcall, J. N., et al. 1993, ApJS, 87, 1

Bahcall, J. N., et al. 1996, ApJ, 457, 19

Barlow, T. A. & Sargent, W. L. W. 1997, AJ, 113, 136

Bergeron, J., Boksenberg, A., Dennefeld, M., Tarenghi, M. 1983, MNRAS, 202, 125

Crenshaw, D. M., Kraemer, S. B., Hutchings, J. B., Danks, A. C., Gull, T. R., Kaiser, M. E., Nelson, C. H., & Weistrop, D. 2000, ApJ, 545, 27

Foltz, C. B., Weymann, R. J., Peterson, B. P., Sun, L., Malkan, M. A., & Chaffee, F. H. 1986, ApJ, 307, 504

Ganguly, R., Eracleous, M., Charlton, J. C., & Churchill, C. W. 1999, AJ, 117, 2594

Ganguly, R., Bond, N. A., Charlton, J. C., Eracleous, M., Brandt, W. N., Churchill, C. W. 2001, ApJ, 549, 133

Halpern, J. P. 1984, ApJ, 281, 90

Hamann, F., Barlow, T. A., Beaver, E. A., Burbidge, E. M., Cohen, R. D., Junkkarinen, V., & Lyons, R. 1995, ApJ, 443, 606

Hamann, F., Barlow, T. A., Junkkarinen, V., & Burbidge, E. M. 1997a, ApJ, 478, 80

Hamann, F., Barlow, T. A., & Junkkarinen, V. 1997b, ApJ, 478, 87

Hamann, F., Barlow, T. A., Cohen, R. D., Junkkarinen, V., & Burbidge, E. M., 1997c, in ASP Conference Ser. 128, Mass Ejection from Active Galactic Nuclei, ed. N. Arav, I. Shlosman, & R. Weymann (San Francisco: ASP), 19

Jannuzi, B. T., et al. 1998, *ApJS*, 118, 1

Maran, S. P., Crenshaw, D. M., Mushotzky, R. F., Reichert, G. A., Carpenter, K. G., Smith, A. M., Hutchings, J. B., & Weymann, R. J. 1996, *ApJ*, 465, 733

Monier, E. M., Mathur, S., Wilkes, B., Elvis, M. 2001, *astro-ph/0102348*

Richards, G. T., York, D. G., Yanny, B., Kollgaard, R. I., Laurent-Muehleisen, S. A., & vanden Berk, D. E. 1999, *ApJ*, 513, 576

Schneider, D. P., et al. 1993, *ApJS*, 87, 45

Shull, J. M., & Sachs, E. R. 1993, *ApJ*, 416, 536

Walter, R., Courvoisier, T. J.-L., Ulrich, M.-H., & Buson, L. M. 1990, *A&A*, 233, 53

Weymann, R. J., Morris, S. L., Gray, M. E., & Hutchings, J. B. 1997, *ApJ*, 483, 717

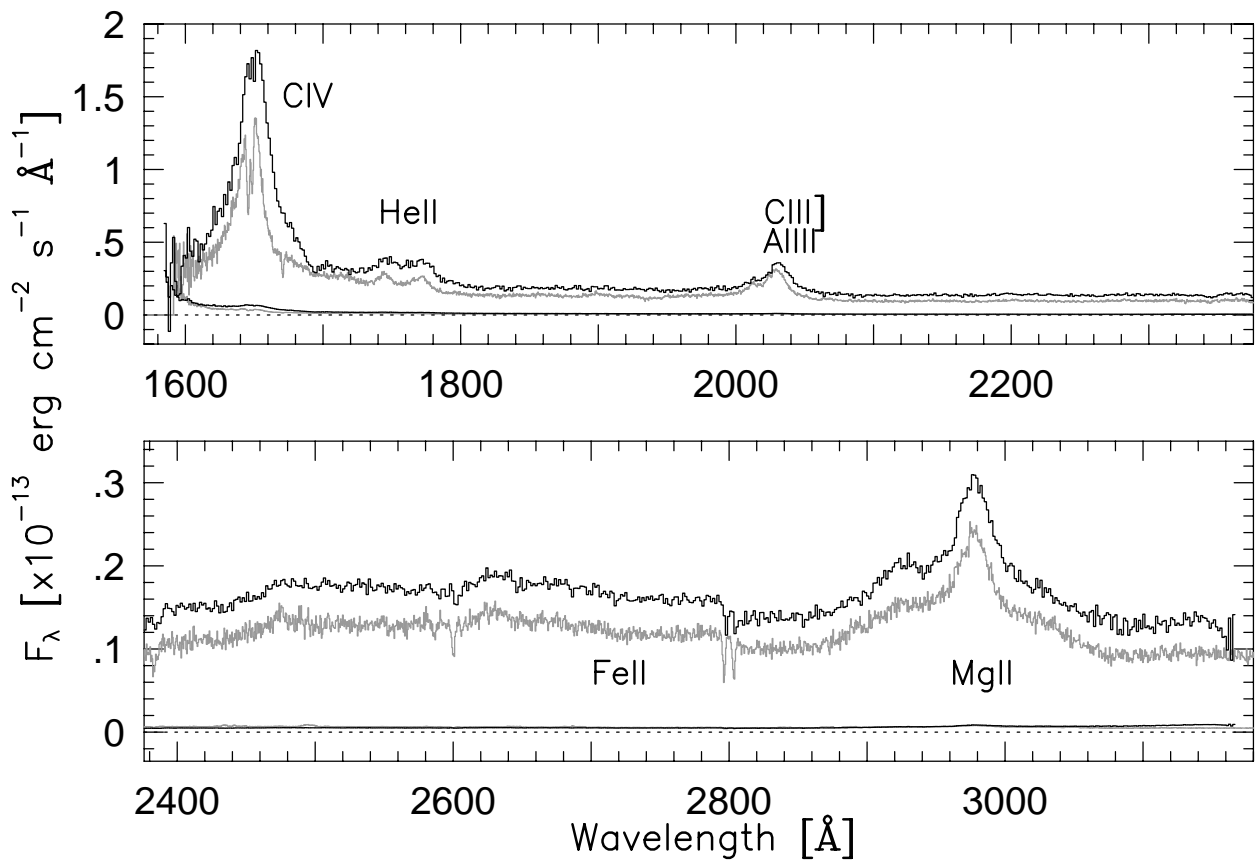


Fig. 1.— STIS-G230L spectrum of MRC 2251-178. The two histograms shown are the STIS spectrum (dark) from 5 November 2000 and FOS spectrum (light) from 2 August 1996 (Monier et al. 2001). The STIS spectrum covers the range 1570–3180 Å. The emission lines covered include C IV, He II, C III], Al III, the Fe II complex, and Mg II. Galactic absorption from Fe II and Mg II as well as a hint of the associated C IV absorber are also present.

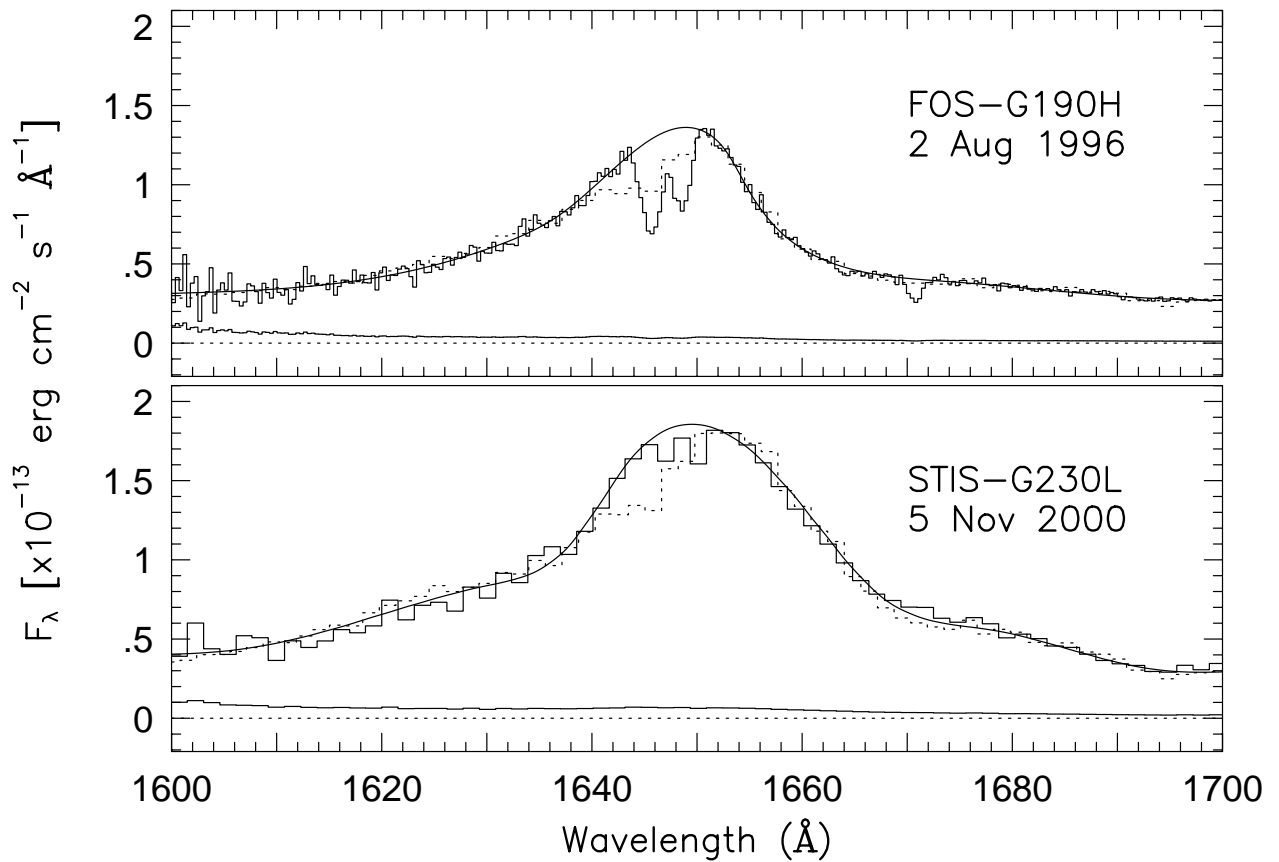


Fig. 2.— Comparison of FOS-G190H and STIS-G230L spectra. In both panels we show the flux density and error spectrum in the region around the C IV emission line. In the top panel we show the FOS-G190H spectrum (solid histogram), the fit to the effective continuum (smooth solid spline), and the expected STIS-G230L spectrum if nothing had varied (dotted histogram). In the bottom panel, we show the observed STIS-G230L spectrum (solid histogram), the fit to the effective continuum (smooth solid spline), and the expected spectrum if no absorber properties changed (dotted histogram). It is clear, to about 10σ confidence, that the associated C IV absorber varied.